

# Material Extrusion Additive Manufacturing of Metal

Subjects: [Metallurgy & Metallurgical Engineering](#)

Contributor: Anchalee MANONUKUL ,

Material extrusion additive manufacturing of metal (metal MEX), which is one of the 3D printing processes, has gained more interests because of its simplicity and economics. Metal MEX process is similar to the conventional metal injection moulding (MIM) process, consisting of feedstock preparation of metal powder and polymer binders, layer-by-layer 3D printing (metal MEX) or injection (MIM) to create green parts, debinding to remove the binders and sintering to create the consolidated metallic parts.

material extrusion

3D printing

fused filament fabrication

metal injection moulding

## 1. Introduction

From the ISO/ASTM 52900, additive manufacturing (AM), usually known as 3D-printing, is a process of joining materials to make parts from 3D model data, usually layer by layer, as opposed to subtractive manufacturing and formative manufacturing methodologies <sup>[1]</sup>. This process has become increasingly popular for various material fabrications, such as ceramic, polymer and metal <sup>[2][3][4][5]</sup>. Many metal AM processes, such as powder bed fusion (PBF), direct energy deposition (DED) and materials extrusion (MEX) can successfully fabricate various metals, e.g., stainless steel <sup>[6][7][8][9]</sup>, titanium alloys <sup>[10][11][12][13]</sup>, nickel alloys <sup>[14][15][16][17][18]</sup>, cobalt <sup>[19][20]</sup> and aluminium alloys <sup>[21][22][23][24][25]</sup>. AM can also provide a high degree of freedom, lightweight design with almost unlimited shape, complexity and a varied range of sizes depending on the printing process <sup>[26]</sup>. In addition, the AM parts are not only limited to prototyping, but can be applied in various technologies, including modelling, pattern-making, tool-making and end-use parts productions with very high growth rates <sup>[27]</sup>. Hence, AM parts can be served in many industries, e.g., biomedical, aerospace and energy applications <sup>[3][28]</sup>. Among the several techniques of metal AM, metal MEX utilises low-cost equipment with simplicity and safety, as neither loose metal powder nor a high-power source is required when compared to other common metal AM processes, i.e., laser powder bed fusion (LPBF) and electron beam powder bed fusion (EPBF) <sup>[9][29]</sup>. During the last decade, this metal MEX process has attracted more attention due to the as-mentioned advantages and the familiarities with conventional polymer 3D printing, which is the metal-fused filament fabrication process (FFF), usually called fused deposition modelling (FDM). **Figure 1** shows the number of publications relating to metal MEX per year and the cumulative number.

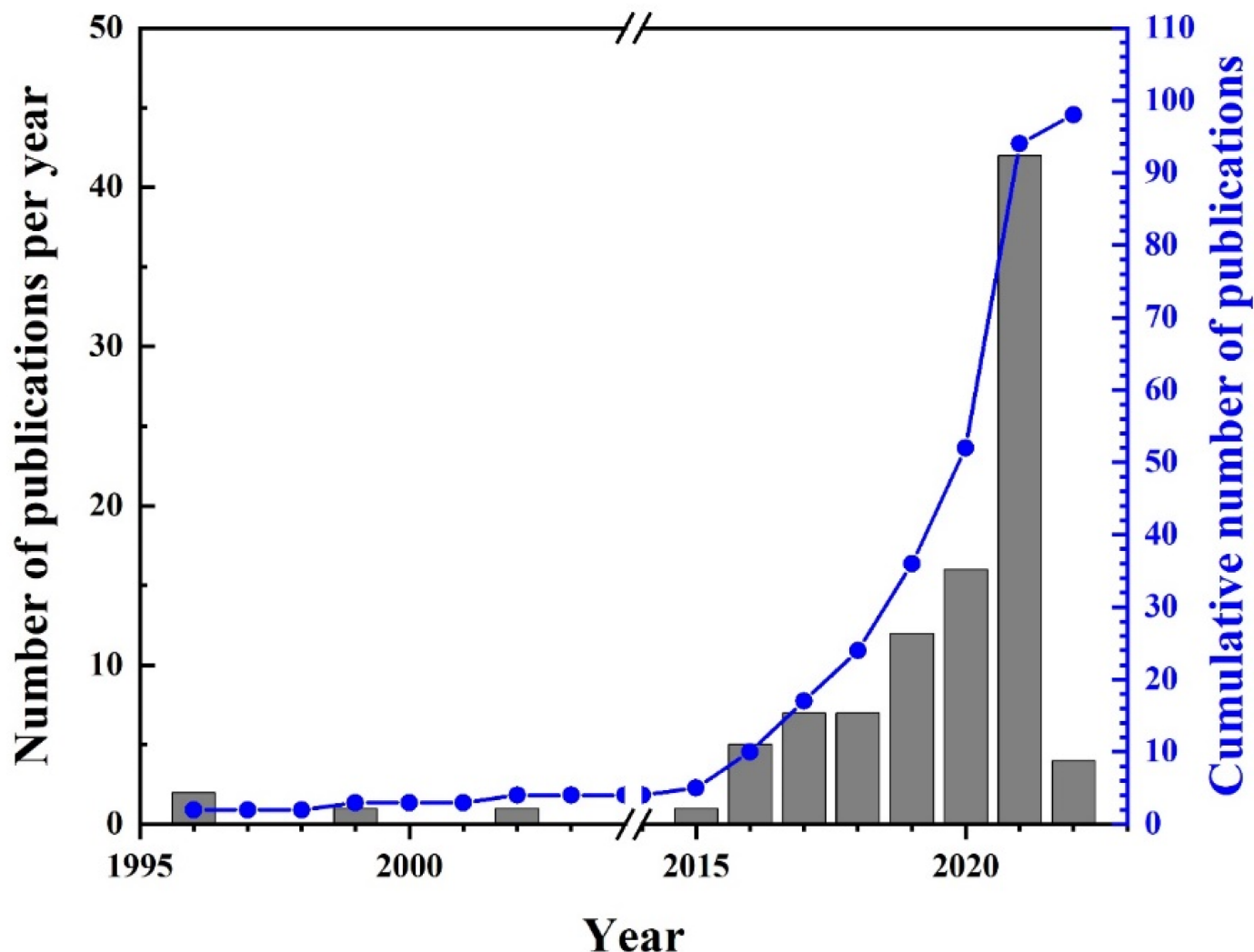
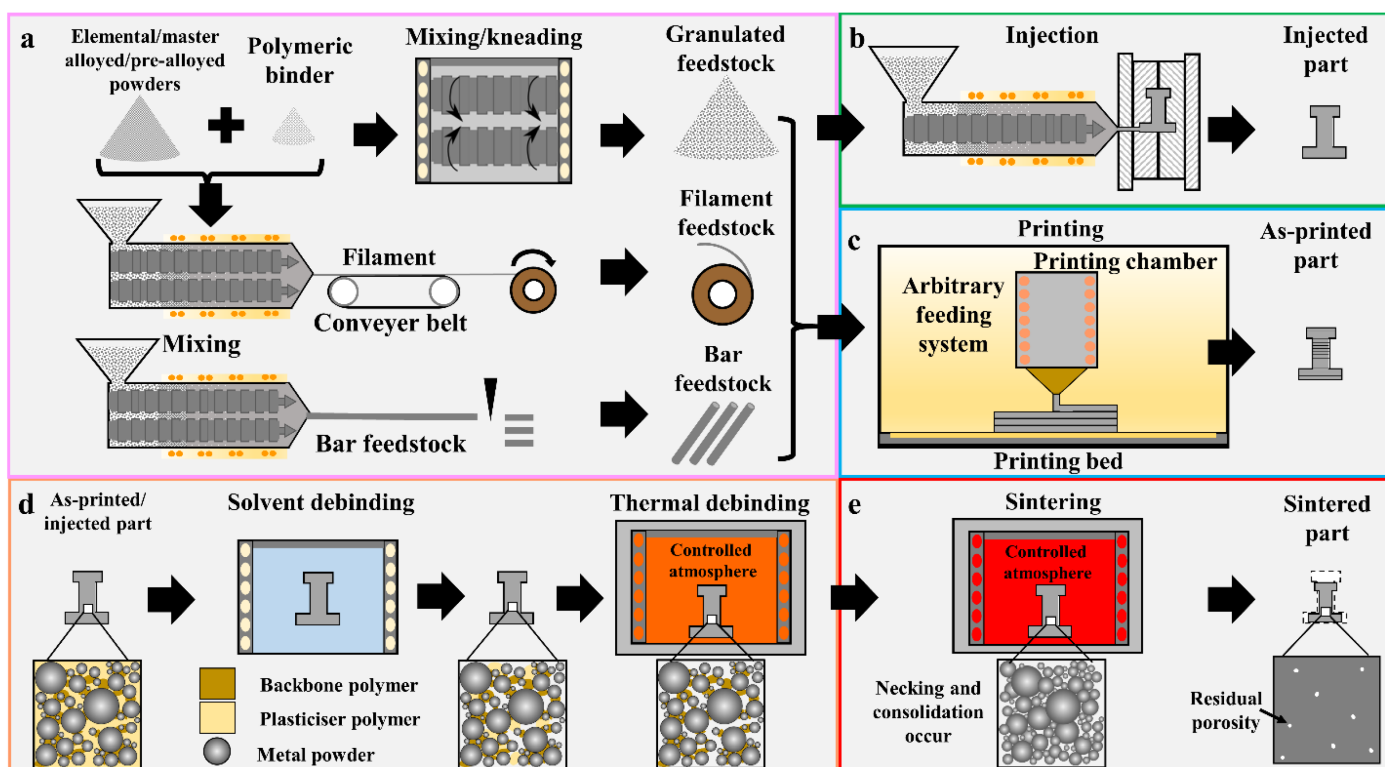


Figure 1. Number of publications relating to the metal MEX from 1996 to February 2022. Data from [\[4\]](#)[\[5\]](#)[\[8\]](#)[\[9\]](#)[\[29\]](#)[\[30\]](#)[\[31\]](#)[\[32\]](#)[\[33\]](#)[\[34\]](#)[\[35\]](#)[\[36\]](#)[\[37\]](#)[\[38\]](#)[\[39\]](#)[\[40\]](#)[\[41\]](#)[\[42\]](#)[\[43\]](#)[\[44\]](#)[\[45\]](#)[\[46\]](#)[\[47\]](#)[\[48\]](#)[\[49\]](#)[\[50\]](#)[\[51\]](#)[\[52\]](#)[\[53\]](#)[\[54\]](#)[\[55\]](#)[\[56\]](#)[\[57\]](#)[\[58\]](#)[\[59\]](#)[\[60\]](#)[\[61\]](#)[\[62\]](#)[\[63\]](#)[\[64\]](#)[\[65\]](#)[\[66\]](#)[\[67\]](#)[\[68\]](#)[\[69\]](#)[\[70\]](#)[\[108\]](#)[\[109\]](#)[\[110\]](#)[\[111\]](#)[\[112\]](#)[\[113\]](#)[\[114\]](#)[\[115\]](#)[\[116\]](#)[\[117\]](#)[\[118\]](#)[\[119\]](#)[\[120\]](#)[\[121\]](#)[\[122\]](#)[\[123\]](#).

The nature of metal MEX is very similar to the conventional metal injection moulding (MIM) [\[124\]](#)[\[125\]](#). The overall MIM and metal MEX processing steps are presented in **Figure 2a,b,d,e** and **Figure 2a,c,d,e**, respectively. The MIM process starts with the mixing of sinterable metal powder with suitable polymeric binders and then granulating the metal-binder mixture into feedstock **Figure 2a**. The feedstock is subsequently injected into a mould to create the injected part, commonly called a “green part” (**Figure 2b**). The polymeric binders are then removed by solvent (optional) and thermal debinding (**Figure 2d**) before the debound parts are sintered in a controlled atmosphere, e.g., H<sub>2</sub>, N<sub>2</sub>, Ar or vacuum atmosphere, to densify the parts (**Figure 2e**). During sintering, necks are formed to bond between adjacent powder particles, consolidation takes place and voids are closed. This causes shrinkage of the sintered part, which in theory should be uniform. However, in practice, the uniformity of shrinkage depends on several factors, e.g., the homogeneity of feedstock and the resultant green parts, geometry, gravity and friction between the parts and sintering tray. Typical MIM shrinkage lies within the range of 12–20% [\[125\]](#)[\[126\]](#)[\[127\]](#). Hence, the mould cavity needs to be oversized to compensate for the shrinkage. After sintering, the density of the MIMed specimen can reach up to 99% of the theoretical density. Hot isostatic pressing (HIP) can be applied, if high

mechanical property and density are required. For the metal MEX, instead of forming the green part by the injection moulding process, it is printed layer by layer (the process in **Figure 2b** is replaced by that in **Figure 2c**) with various forms of feedstock, i.e., granule, bar and filament, depending on the printer. After printing, the subsequent debinding and sintering steps (**Figure 2d,e**) may be slightly different from the MIM process due to the differences in compositions of binders and the metal powder fraction (usually named “solid loading”), metal powder size and its distribution. The shrinkage of the sintered metal MEX part is generally higher than for MIM parts because the metal MEX feedstock usually has higher binder content (lower solid loading) than MIM so that the metal MEX feedstock is printable and can be easily handled. Therefore, dimensions of the CAD model need to be carefully compensated to acquire the required dimension after sintering. The sintered density and mechanical properties of the metal MEX part are theoretically lower than those of MIM due to the voids between deposited paths generated during printing [8]. Thereby, the print strategy, which can generate not only such voids but also deflection and incomplete weld in polymer 3D-print parts [128][129][130], needs to be carefully controlled for metal MEX before progressing to the debinding and sintering.



**Figure 2.** Comparison of material extrusion additive manufacturing of metal (**a,c,d,e**) and metal injection moulding (**a,b,d,e**).

## 2. Material Extrusion Additive Manufacturing of Metal (Metal MEX)

In metal MEX, the feedstock composing of metal powder and polymeric binders is heated until the filament is softened and can be extruded through a printing nozzle. The printed material is then deposited on the printing bed,

which is heated to increase adhesion between the printed parts and the printing bed so that the 3D part is created layer-by-layer following the CAD model [131]. This metal MEX process can also fabricate multi-material 3D parts, when a printer has more than one printing head or feeding system. Depending on the feeding system of the printer, the metal MEX process can be classified into three types, as presented in **Figure 3**, which are (a) screw-based, (b) plunger-based and (c) filament-based types [132]. After printing, the as-printed parts require to be debound and sintered in a similar manner to those in the MIM processing steps, as presented in **Figure 2d,e**.

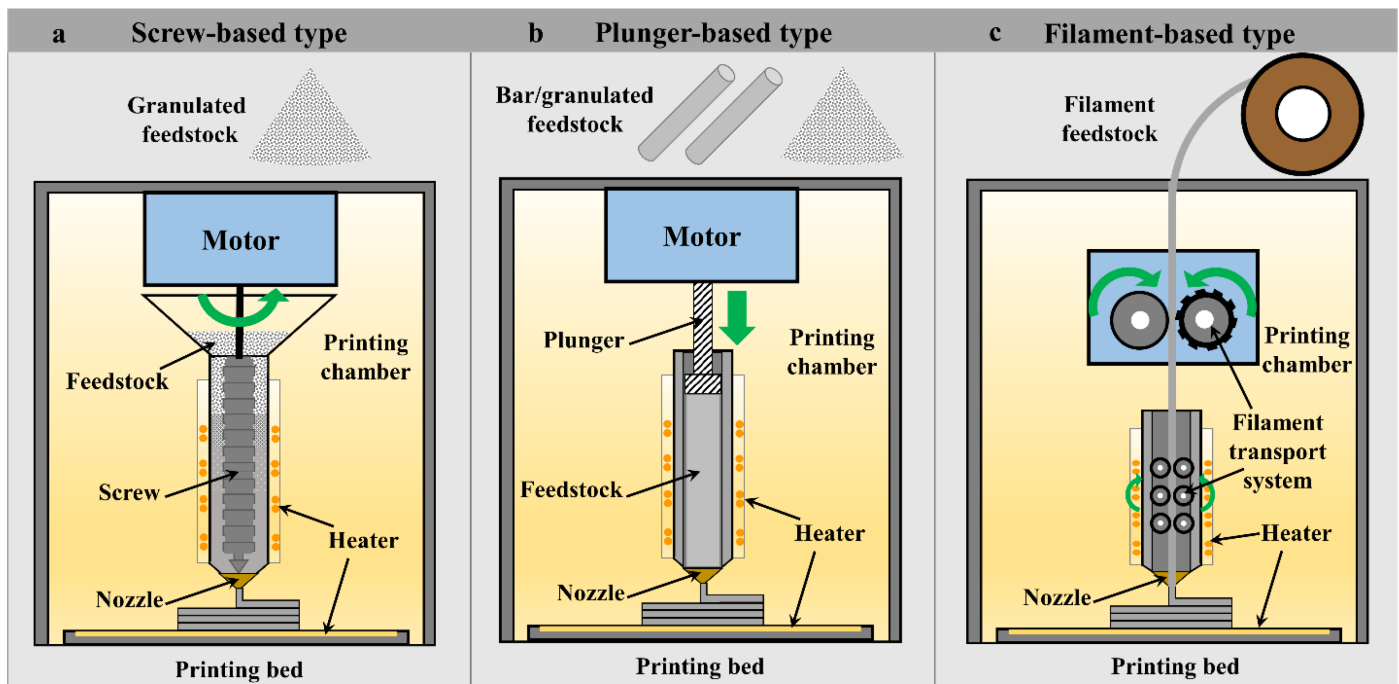


**Figure 3.** Types of material extrusion additive manufacturing classified by feeding system: (a) screw-based, (b) plunger-based and (c) filament-based types.

- **Screw-based MEX (SB)**

High quality metal filament and bar feedstocks are still very limited in alloy selection. Hence, screw-based MEX is currently the most versatile material extrusion system in term of material selection. Screw-based MEX uses the granulated feedstock in a similar form as MIM, hence all alloys for MIM feedstocks are applicable. The feedstock will be transported by screw rotation [132] and simultaneously heated by heating elements to a temperature above the glass transition temperature of the polymer binder. The softened material will be deposited through the nozzle in a pattern that follows the CAD design, as presented in **Figure 3a**. The advantages of this type over the latter two processes, which are plunger- (**Figure 3b**) and filament- (**Figure 3c**) based types are high productivity due to a continuous filling system and no requirement for an additional processing step for bar or filament preparation. In addition, high solid loading equivalent to that employed in MIM can be used. This process provides the best available feedstock filling system, which can continuously feed without interruption during printing, as the feedstock in the system is replenished. This results in printing time reduction, as neither printing stoppage during feedstock replenishment nor feedstock re-heating to the printing temperature is mandatory. There is also no need for

additional equipment for bar or filament preparation and know-how to produce and handle feedstocks, especially filament feedstock, which is commonly brittle and difficult to handle. The size of the granulated feedstock needs to be controlled (<5 mm) to obtain stability during printing and reduce printing defects generated by air entrapment [133]. As reported by Singh et al. [85], the granule feedstock, sized from 3 to 5 mm, can provide relative sintered density up to 94% after sintering. Likewise, Lieberwirth et al. [41] reported that a granule size of 3 mm could be readily printed, yielding good appearance. Too large granulated feedstock may not be evenly and properly softened in the feeding system. Too small granulated feedstock may cause blocking at the hopper. Any printed mono-material green parts with defects or mistakes can be easily re-used by crushing and sieving before feeding back into the printer hopper, similar to the re-use of MIM injected parts with defects and all runner systems [134]. The other two types of printing systems need an additional bar or filament preparation step. The stabilisation of the screw system is still challenging to fabricate the 3D part, as it is difficult to control the flow rate of the material to be constant due to the trapped air inside the softened material. Moreover, the strength and stability of the printing system are also required during printing due to the high viscosity of the feedstock. The well-known commercially available screw-based MEX systems are proposed by AIM3D GmbH with a “ceramic extrusion modelling” system (CEM) [135] and Pollen AM, Ltd. With a “pallet additive manufacturing” system (PAM) [136], in which multi-material parts, such as both ceramic and metal, can be fabricated by using general powder injection moulding feedstocks. **Figure 4a** shows the AIM3D printer and the schematic representing the printing, while **Figure 4b** shows the feedstock and the microstructure of the feedstock utilised for the AIM3D printer. Recently, pallet extrusion system has been introduced by Direct3D, which supplies both a screw-based printer and only a screw-based print head that can be applied with a suitable 3D printer [137]. In addition, most MIM manufacturers will prefer to use their current MIM feedstock so that they can use their current debinding and sintering systems. Hence, the implementation of metal MEX will be easier, smoother, faster and more economical for MIM manufacturers.

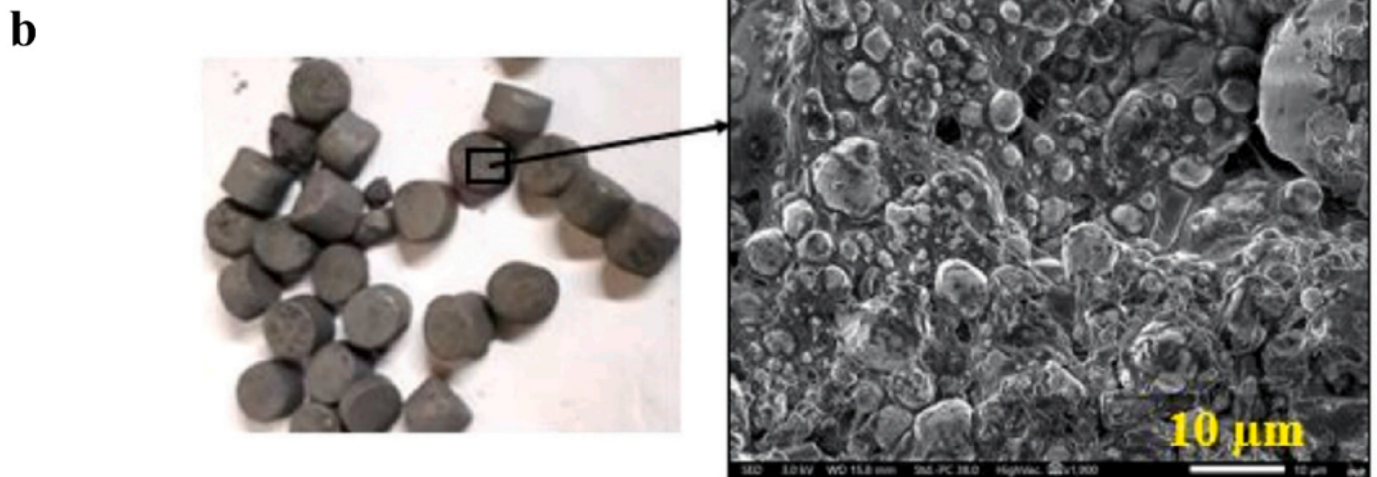
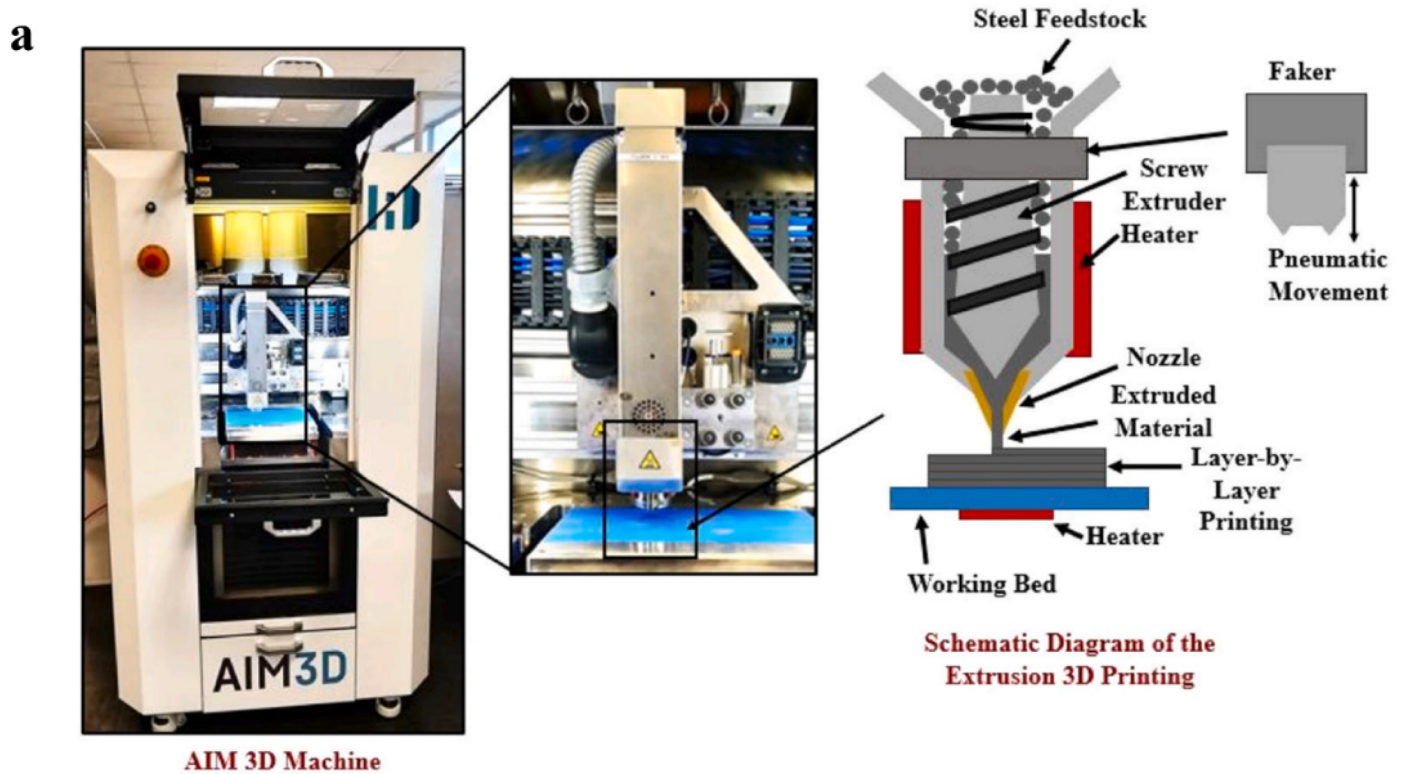


**Figure 4.** (a) AIM3D printer and the schematic representing the printing and (b) low and high magnification of the 17-4PH stainless steel granulated feedstock utilised for the printer [92].

- **Plunger-based MEX (PB)**

The plunger-based MEX utilises bar or granulated feedstock to feed to the nozzle of the plunger system. Desktop Metal, Inc. [138] proposes the plunger-based system using circular-bar feedstock, called “bound deposition modelling” (BMD), in which the bar feedstock will be fed by a cartridge into a heated sleeve. The feedstock is then pushed through the nozzle for layer-by-layer printing by the plunger following the CAD design as presented in **Figure 3b**. One of the main advantages of this system is the high material handling ability, which is significantly easier than the filament feedstock. Besides, the solid loading of the bar feedstock can be higher than the filament-

based printers and comparable to the MIM feedstock. However, one of the main disadvantages of the plunger-based system when compared to the screw-based one is the additional step of bar feedstock preparation. The bar feedstock can be prepared by extruding the mixture of metal powder and polymer binders and cut to size, as shown in **Figure 2a**. Furthermore, print discontinuity occurs when the feedstock is required to be replenished. To overcome this disadvantage, Giberti et al. proposed an in-house developed machine, as shown in **Figure 5a**, combining a screw-based to feed the MIM feedstock and plunger system to push the feedstock through the nozzle [36]. However, at the end of the plunger stroke, the plunger still requires reversing to receive the softened feedstock from the screw-based plasticiser. Hence, the discontinuity is minimised but remained. As the injection unit is stationary, the deposited path will be printed on the printing bed of a 5-axes parallel kinematics machine (PKM). Hence, parts can be printed with minimal support materials. In 2020, Waalkes et al. proposed an in-house plunger-based printer, as presented in **Figure 5b**, which can fabricate the 3D part of Ti-6Al-4V using commercial MIM feedstock [61]. This in-house system successfully fabricates the as-printed parts with a good appearance and high stability. Moreover, the production cost of the machine is claimed to be close to the open polymer filament-based systems (5–10 k€) [61]. These in-house developed plunger-based printers provide the ability to use MIM feedstock. This increases the flexibility in material selection. In addition, there is no need for further feedstock preparation into filament form.

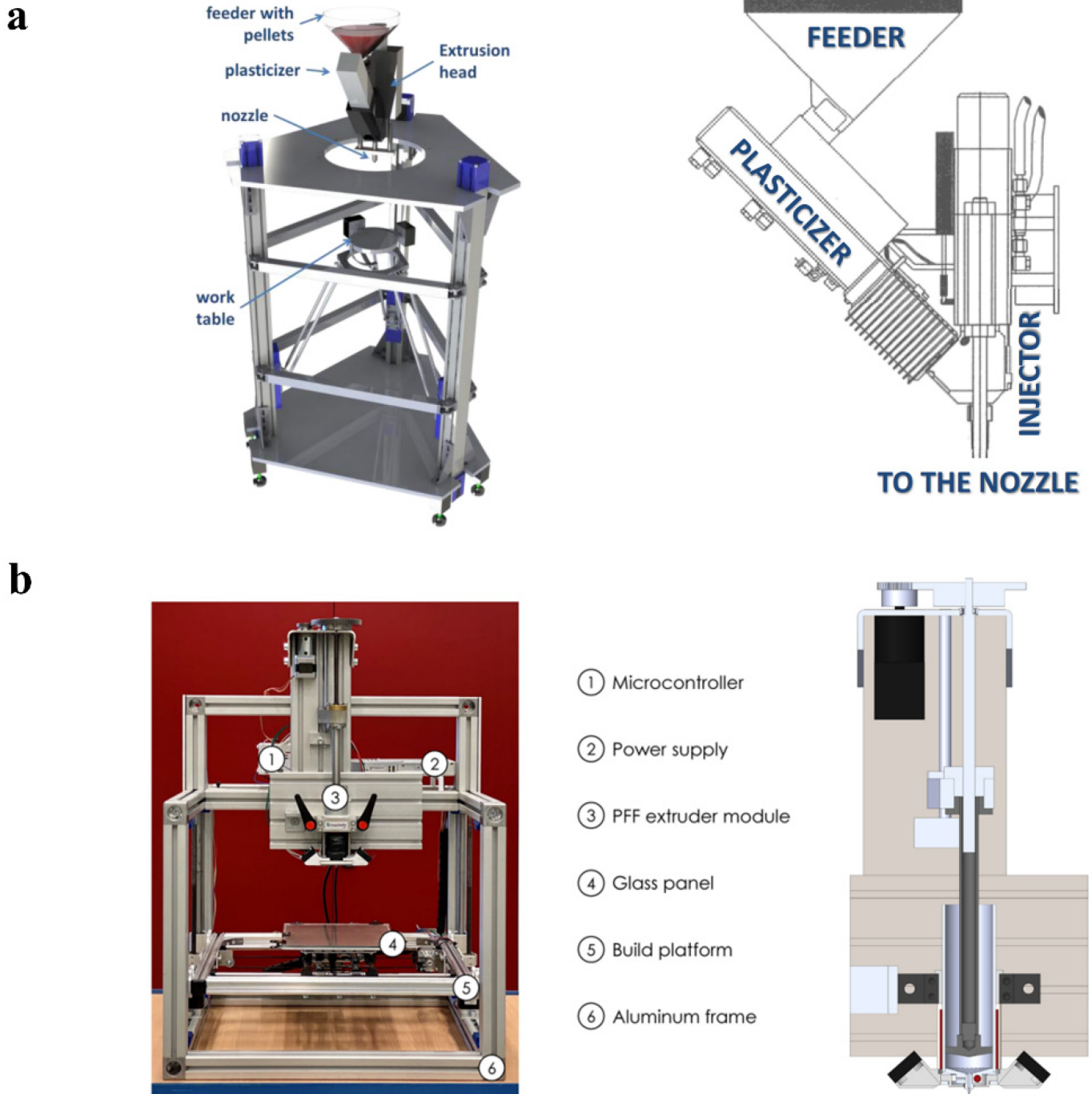


**Figure 5.** (a) In-house developed machine and their components with the extrusion unit combining a screw-based (plasticiser) to feed the feedstock and plunger system to inject the feedstock through the nozzle [36] and (b) in-house developed plunger-based printer and their components with the schematic of the extruder unit [61].

- **Filament-based MEX (FB)**

Filament-based type is the most popularly and widely used metal MEX process. It is known by many terms, such as “fused deposition modelling” (FDM), first developed by Stratasys, Ltd. (Eden Prairie, MN, USA and Rehovot, Israel) for polymer [139]; “fused filament fabrication” (FFF) or “atomic diffusion additive manufacturing” (ADAM)

proposed by Markforged, Inc., Watertown, MA, USA [140]. At the beginning, this process was usually used for rapid prototyping; however, it can currently be used for tooling and end-user part fabrication [50][140][141]. The filament of metal MEX composed of the metal powder and polymeric binder is fed by the filament transport system to the heating element and heated nozzle so that the filament will be softened and extruded to the printing bed layer-by-layer following the CAD design as illustrated in **Figure 3c**. The advantages of this filament-based process are safety, simplicity and familiarity of the process, and its low-cost equipment because the general desktop polymer 3D printer is used with the metal MEX filament. The high volume fraction of metal in the filament results in a high wear rate of the printing nozzle; hence, a special ruby or hardened steel nozzle should be utilised to produce a stable flow of the filament, prolong the nozzle life [142] and reduce contamination. The main disadvantage of this process is the need for filament production, which requires single/twin screws or plunger extrusion equipment for filament fabrication [34][52], plus special know-how, e.g., the selection of appropriate binder types, suitable mixing procedure and the filament fabrication technique [31]. The filament properties are very important to the final shape, size, dimension and properties in both as-printed and as-sintered stages. Appropriate binders must be selected to provide the desired properties in the filament. The filament should have high strength and stiffness so that the filament can be driven by the roller or gear without breaking and bulking [31][143][144]. The high bonding strength of the metal powder and binders of the filament can provide strong weldability between deposit paths. In addition, the filament should have high flexural strength and stiffness so that the filament can be spooled and handled with ease [31]. The filament will be brittle if too-high solid loading is used [145]. Very careful handling of the filament is needed with an extra heater to reduce the brittleness of the filament and to reset the memory shape [56][64][146]. The filament must have no porosity, shape consistency and uniform distribution of the metal powder, including as high as possible of solid loading to minimise shrinkage [94]. The above factors directly influence the printing, debinding and sintering processes, which can be prone to generate many defects. High quality sintered parts can be achieved if these factors and the processes are correctly controlled. Examples of commercially available filaments are Ultrafuse 316L<sup>®</sup> by BASF SE [147], Filamet<sup>®</sup> by Virtual foundry [146] and 316L metal filament by Anycubic [148], which provide high-quality metal filaments, together with the suggested suitable range of processing parameters. The cross section of commercially available filament by BASF (**Figure 6a**), Virtual foundry (**Figure 6b**), including the filament specially developed for MetalX by Markforged, Inc. (**Figure 6b**) shows high fraction of the metal powder. It is noted that the Ultrafuse 316L filament uses polymer skin (**Figure 6a**) to case the filament to increase the flexibility of the filament [4], while the Filamet and Anycubic filament use binder with high flexibility and lower solid loading [48][146].

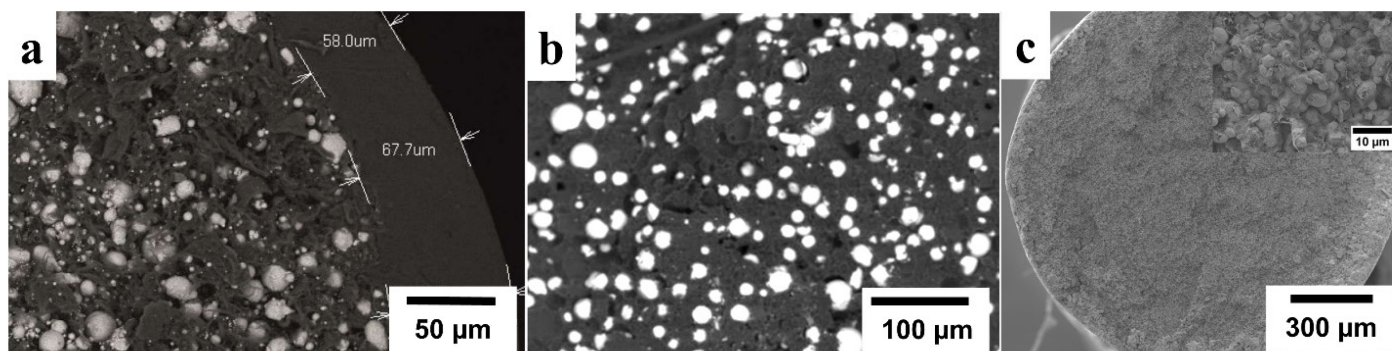


**Figure 6.** Cross-sectional view of the commercial filaments—(a) Ultrafuse by BASF [4], showing polymer skin surrounding mixing of polymer and metal powder, (b) 316L metal filament by Virtual foundry [72] and (c) 17-4PH stainless steel filament for MetalX system by Markforged, Inc [8].

## References

1. ISO/ASTM 52900:2021; Standard Terminology for Additive Manufacturing—General Principles—Terminology. ASTM International: West Conshohocken, PA, USA, 2021.
2. Ngo, T.D.; Kashani, A.; Imbalzano, G.; Nguyen, K.T.Q.; Hui, D. Additive manufacturing (3D printing): A review of materials, methods, applications and challenges. *Compos. Part B Eng.* 2018, 143, 172–196.
3. Frazier, W.E. Metal additive manufacturing: A review. *J. Mater. Eng. Perform.* 2014, 23, 1917–1928.
4. Gonzalez-Gutierrez, J.; Cano, S.; Schuschnigg, S.; Kukla, C.; Sapkota, J.; Holzer, C. Additive manufacturing of metallic and ceramic components by the material extrusion of highly-filled polymers: A review and future perspectives. *Materials* 2018, 11, 840.
5. Nurhudan, A.I.; Supriadi, S.; Whulanza, Y.; Saragih, A.S. Additive manufacturing of metallic based on extrusion process: A review. *J. Manuf. Processes* 2021, 66, 228–237.
6. Suryawanshi, J.; Prashanth, K.G.; Ramamurty, U. Mechanical behavior of selective laser melted 316L stainless steel. *Mater. Sci. Eng. A* 2017, 696, 113–121.
7. Murr, L.E.; Martinez, E.; Hernandez, J.; Collins, S.; Amato, K.N.; Gaytan, S.M.; Shindo, P.W. Microstructures and properties of 17-4 PH stainless steel fabricated by Selective Laser Melting. *J. Mater. Res. Technol.* 2012, 1, 167–177.
8. Suwanpreecha, C.; Seensattayawong, P.; Vadhanakovint, V.; Manonukul, A. Influence of specimen layout on 17-4PH (AISI 630) alloys fabricated by low-cost additive manufacturing. *Metall. Mater. Trans. A* 2021, 52, 1999–2009.
9. Gong, H.; Snelling, D.; Kardel, K.; Carrano, A. Comparison of stainless steel 316L parts made by FDM- and SLM-based additive manufacturing processes. *JOM* 2019, 71, 880–885.
10. Barba, D.; Alabort, C.; Tang, Y.T.; Viscasillas, M.J.; Reed, R.C.; Alabort, E. On the size and orientation effect in additive manufactured Ti-6Al-4V. *Mater. Des.* 2020, 186, 108235.
11. Suwanpreecha, C.; Alabort, E.; Tang, Y.T.; Panwisawas, C.; Reed, R.C.; Manonukul, A. A novel low-modulus titanium alloy for biomedical applications: A comparison between selective laser melting and metal injection moulding. *Mater. Sci. Eng. A* 2021, 812, 141081.

12. Brandl, E.; Palm, F.; Michailov, V.; Viehweger, B.; Leyens, C. Mechanical properties of additive manufactured titanium (Ti–6Al–4V) blocks deposited by a solid-state laser and wire. *Mater. Des.* 2011, 32, 4665–4675.
13. Song, B.; Kenel, C.; Dunand, D.C. 3D ink-extrusion printing and sintering of Ti, Ti-TiB and Ti-TiC microlattices. *Addit. Manuf.* 2020, 35, 101412.
14. Trosch, T.; Strößner, J.; Völkl, R.; Glatzel, U. Microstructure and mechanical properties of selective laser melted Inconel 718 compared to forging and casting. *Mater. Lett.* 2016, 164, 428–431.
15. Pleass, C.; Jothi, S. Influence of powder characteristics and additive manufacturing process parameters on the microstructure and mechanical behaviour of Inconel 625 fabricated by Selective Laser Melting. *Addit. Manuf.* 2018, 24, 419–431.
16. Smith, D.H.; Bicknell, J.; Jorgensen, L.; Patterson, B.M.; Cordes, N.L.; Tsukrov, I.; Knezevic, M. Microstructure and mechanical behavior of direct metal laser sintered Inconel alloy 718. *Mater. Charact.* 2016, 113, 1–9.
17. Pérez-Ruiz, J.D.; Marin, F.; Martínez, S.; Lamikiz, A.; Urbikain, G.; López de Lacalle, L.N. Stiffening near-net-shape functional parts of Inconel 718 LPBF considering material anisotropy and subsequent machining issues. *Mech. Syst. Signal Process.* 2022, 168, 108675.
18. Pérez-Ruiz, J.D.; de Lacalle, L.N.L.; Urbikain, G.; Pereira, O.; Martínez, S.; Bris, J. On the relationship between cutting forces and anisotropy features in the milling of LPBF Inconel 718 for near net shape parts. *Int. J. Mach. Tools Manuf.* 2021, 170, 103801.
19. Darvish, K.; Chen, Z.W.; Phan, M.A.L.; Pasang, T. Selective laser melting of Co-29Cr-6Mo alloy with laser power 180–360W: Cellular growth, intercellular spacing and the related thermal condition. *Mater. Charact.* 2018, 135, 183–191.
20. Cloots, M.; Kunze, K.; Uggowitzer, P.J.; Wegener, K. Microstructural characteristics of the nickel-based alloy IN738LC and the cobalt-based alloy Mar-M509 produced by selective laser melting. *Mater. Sci. Eng. A* 2016, 658, 68–76.
21. Glerum, J.A.; Kenel, C.; Sun, T.; Dunand, D.C. Synthesis of precipitation-strengthened Al-Sc, Al-Zr and Al-Sc-Zr alloys via selective laser melting of elemental powder blends. *Addit. Manuf.* 2020, 36, 101461.
22. Griffiths, S.; Rossell, M.D.; Croteau, J.; Vo, N.Q.; Dunand, D.C.; Leinenbach, C. Effect of laser rescanning on the grain microstructure of a selective laser melted Al-Mg-Zr alloy. *Mater. Charact.* 2018, 143, 34–42.
23. Olakanmi, E.O. Selective laser sintering/melting (SLS/SLM) of pure Al, Al–Mg, and Al–Si powders: Effect of processing conditions and powder properties. *J. Mater. Process. Technol.* 2013, 213, 1387–1405.

24. Martin, J.H.; Yahata, B.D.; Hundley, J.M.; Mayer, J.A.; Schaedler, T.A.; Pollock, T.M. 3D printing of high-strength aluminium alloys. *Nature* 2017, 549, 365–369.
25. Michi, R.A.; Plotkowski, A.; Shyam, A.; Dehoff, R.R.; Babu, S.S. Towards high-temperature applications of aluminium alloys enabled by additive manufacturing. *Int. Mater. Rev.* 2021; 1–48, ahead-of-print.
26. Khorasani, M.; Ghasemi, A.; Rolfe, B.; Gibson, I. Additive manufacturing a powerful tool for the aerospace industry. *Rapid Prototyp. J.* 2021, 28, 87–100.
27. Caffrey, T.; Wohlers, T.; Campbell, I. Executive Summary of the Wohlers Report 2016; Loughborough University: Loughborough, UK, 2016.
28. Buchanan, C.; Gardner, L. Metal 3D printing in construction: A review of methods, research, applications, opportunities and challenges. *Eng. Struct.* 2019, 180, 332–348.
29. Riecker, S.; Clouse, J.; Studnitzky, T.; Andersen, O.; Kieback, B. Fused Deposition Modeling- Opportunities for Cheap Metal AM. In Proceedings of the World PM2016 Congress & Exhibition, Hamburg, Germany, 9–13 October 2016.
30. Rane, K.; Strano, M. A comprehensive review of extrusion-based additive manufacturing processes for rapid production of metallic and ceramic parts. *Adv. Manuf.* 2019, 7, 155–173.
31. Agarwala, M.; van Weeren, R.; Bandyopadhyay, A.; Safari, A.; Danforth, S.; Priedeman, W. Filament feed materials for fused deposition processing of ceramics and metals. In International Solid Freeform Fabrication Symposium Proceedings; University of Texas: Austin, TX, USA, 1996.
32. Agarwala, M.; van Weeren, R.; Bandyopadhyay, A.; Whalen, P.; Safari, A.; Danforth, S. Fused deposition of ceramics and metals: An overview. In International Solid Freeform Fabrication Symposium Proceedings; University of Texas: Austin, TX, USA, 1996.
33. Wu, G.; Langrana, N.A.; Rangarajan, S.; McCuiston, R.; Sadanji, R.; Danforth, S.; Safari, A. Fabrication of metal components using FDMet: Fused deposition of metals. In International Solid Freeform Fabrication Symposium Proceedings; University of Texas: Austin, TX, USA, 1996.
34. Wu, G.; Langrana, N.A.; Sadanji, R.; Danforth, S. Solid freeform fabrication of metal components using fused deposition of metals. *Mater. Des.* 2002, 23, 97–105.
35. Burkhardt, C.; Freigassner, P.; Weber, O.; Imgrund, P.; Hampel, S. Fused filament fabrication (FFF) of 316L green parts for the MIM process. In Proceedings of the World PM2016 Congress & Exhibition, Hamburg, Germany, 9–13 October 2016.
36. Giberti, H.; Strano, M.; Annoni, M. An innovative machine for Fused Deposition Modeling of metals and advanced ceramics. In MATEC Web of Conferences; EDP Sciences: Les Ulis, France, 2016; Volume 43, p. 03003.

37. Kukla, C.; Duretek, I.; Schuschnigg, S.; Gonzalez-Gutierrez, J.; Holzer, C. Properties for PIM feedstocks used in fused filament fabrication. In Proceedings of the World PM2016 Congress & Exhibition, Hamburg, Germany, 9–13 October 2016.
38. Gonzalez-Gutierrez, J.; Godec, D.; Kukla, C.; Schlauf, T.; Burkhardt, C.; Holzer, C. Shaping, debinding and sintering of steel components via fused filament fabrication. In Proceedings of the 16th International Scientific Conference on Production Engineering CIM 2017, Zadar, Croatia, 8–10 June 2017.
39. Kukla, C.; Gonzalez-Gutierrez, J.; Cano, S.; Hampel, S.; Burkhardt, C.; Moritz, T.; Holzer, C. Fused filament fabrication (FFF) of PIM feedstocks. In Proceedings of the VI Congreso Nacional de Pulvimetalurgia y I Congreso Iberoamericano de Conference, Ciudad Real, Spain, 7–9 June 2017.
40. Kukla, C.; Gonzalez-Gutierrez, J.; Duretek, I.; Schuschnigg, S.; Holzer, C. Effect of particle size on the properties of highly-filled polymers for fused filament fabrication. In AIP Conference Proceedings; AIP Publishing: New York, NY, USA, 2017; Volume 1914, p. 190006.
41. Lieberwirth, C.; Harder, A.; Seitz, H. Extrusion based additive manufacturing of metal parts. *J. Mech. Eng. Autom.* 2017, 7, 79–83.
42. Condruz, M.R.; Paraschiv, A.; Puscasu, C. Heat treatment influence on hardness and microstructure of ADAM manufactured 17-4 PH. *Turbo* 2018, 5, 39–45.
43. Gonzalez-Gutierrez, J.; Godec, D.; Guráň, R.; Spoerk, M.; Kukla, C.; Holzer, C. 3D printing conditions determination for feedstock used in fused filament fabrication (FFF) of 17-4PH stainless steel parts. *Metalurgija* 2018, 57, 117–120.
44. Gonzalez-Gutierrez, J.; Cano, S.; Schuschnigg, S.; Holzer, C.; Kukla, C. Highly-filled polymers for fused filament fabrication. *Leobener Kunstst.-Kolloqu.* 2018, 27, 93–104.
45. Damon, J.; Dietrich, S.; Gorantla, S.; Popp, U.; Okolo, B.; Schulze, V. Process porosity and mechanical performance of fused filament fabricated 316L stainless steel. *Rapid Prototyp. J.* 2019, 25, 1319–1327.
46. Fidan, S.T.I. Dimensional analysis of metal powder infused filament-low cost metal 3D printing. In International Solid Freeform Fabrication Symposium Proceedings; University of Texas: Austin, TX, USA, 2019; pp. 533–541.
47. Galati, M.; Minetola, P. Analysis of density, roughness, and accuracy of the Atomic Diffusion Additive Manufacturing (ADAM) process for metal parts. *Materials* 2019, 12, 4122.
48. Gante Lokesha Renukaradhya, K. Metal Filament 3D Printing of SS316L: Focusing on the Printing Process. Master Thesis's, KTH Royal Institute of Technology, Stockholm, Sweden, 2019.

49. Gonzalez-Gutierrez, J.; Arbeiter, F.; Schlauf, T.; Kukla, C.; Holzer, C. Tensile properties of sintered 17-4PH stainless steel fabricated by material extrusion additive manufacturing. *Mater. Lett.* 2019, 248, 165–168.
50. Lengauer, W.; Duretek, I.; Fürst, M.; Schwarz, V.; Gonzalez-Gutierrez, J.; Schuschnigg, S.; Kukla, C.; Kitzmantel, M.; Neubauer, E.; Lieberwirth, C.; et al. Fabrication and properties of extrusion-based 3D-printed hardmetal and cermet components. *Int. J. Refract. Met. Hard Mater.* 2019, 82, 141–149.
51. Terry, S.M. *Innovating the Fused Filament Fabrication Process Metal Powder Polylactic Acid Printing*; Tennessee Technological University: Cookeville, TN, USA, 2019.
52. Thompson, Y.; Gonzalez-Gutierrez, J.; Kukla, C.; Felfer, P. Fused filament fabrication, debinding and sintering as a low cost additive manufacturing method of 316L stainless steel. *Addit. Manuf.* 2019, 30, 100861.
53. Ait-Mansour, I.; Kretzschmar, N.; Chekurov, S.; Salmi, M.; Rech, J. Design-dependent shrinkage compensation modeling and mechanical property targeting of metal FFF. *Prog. Addit. Manuf.* 2020, 5, 51–57.
54. Godec, D.; Cano, S.; Holzer, C.; Gonzalez-Gutierrez, J. Optimization of the 3D printing parameters for tensile properties of specimens produced by Fused Filament Fabrication of 17-4PH stainless steel. *Materials* 2020, 13, 774.
55. Korotchenko, A.; Khilkov, D.; Tverskoy, M.; Khilkova, A. Use of additive technologies for metal injection molding. *Eng. Solid Mech.* 2020, 8, 143–150.
56. Kurose, T.; Abe, Y.; Santos, M.V.; Kanaya, Y.; Ishigami, A.; Tanaka, S.; Ito, H. Influence of the layer directions on the properties of 316L stainless steel parts fabricated through fused deposition of metals. *Materials* 2020, 13, 2493.
57. Liu, B.; Wang, Y.; Lin, Z.; Zhang, T. Creating metal parts by Fused Deposition Modeling and sintering. *Mater. Lett.* 2020, 263, 127252.
58. Niemelä, M. *Experimental Strength Tests with Metal X*. Bachelor's Thesis, Vaasan Ammattikorkeakoulu University of Applied Sciences, Vaasa, Finland, 2020.
59. Singh, P.; Balla, V.K.; Tofangchi, A.; Atre, S.V.; Kate, K.H. Printability studies of Ti-6Al-4V by metal fused filament fabrication (MF3). *Int. J. Refract. Met. Hard Mater.* 2020, 91, 105249.
60. Singh, P.; Shaikh, Q.; Balla, V.K.; Atre, S.V.; Kate, K.H. Estimating powder-polymer material properties used in design for Metal Fused Filament Fabrication (DfMF 3). *JOM* 2020, 72, 485–495.
61. Waalkes, L.; Längerich, J.; Holbe, F.; Emmelmann, C. Feasibility study on piston-based feedstock fabrication with Ti-6Al-4 V metal injection molding feedstock. *Addit. Manuf.* 2020, 35, 101207.

62. Watson, A.; Belding, J.; Ellis, B.D. Characterization of 17-4 PH Processed via Bound Metal Deposition (BMD); Springer International Publishing: Cham, Switzerland, 2020.
63. Zhang, Y.; Bai, S.; Riede, M.; Garratt, E.; Roch, A. A comprehensive study on Fused Filament Fabrication of Ti-6Al-4V structures. *Addit. Manuf.* 2020, 34, 101256.
64. Abe, Y.; Kurose, T.; Santos, M.V.; Kanaya, Y.; Ishigami, A.; Tanaka, S.; Ito, H. Effect of layer directions on internal structures and tensile properties of 17-4PH stainless steel parts fabricated by Fused Deposition of metals. *Materials* 2021, 14, 243.
65. Alkindi, T.; Alyammahi, M.; Susantyoko, R.A.; Atatreh, S. The effect of varying specimens' printing angles to the bed surface on the tensile strength of 3D-printed 17-4PH stainless-steels via metal FFF additive manufacturing. *MRS Commun.* 2021, 11, 1–7.
66. Caminero, M.Á.; Romero, A.; Chacón, J.M.; Núñez, P.J.; García-Plaza, E.; Rodríguez, G.P. Additive manufacturing of 316L stainless-steel structures using fused filament fabrication technology: Mechanical and geometric properties. *Rapid Prototyp. J.* 2021, 27, 583–591.
67. Costa, J.; Sequeiros, E.; Vieira, M.T.; Vieira, M. Additive manufacturing: Material extrusion of metallic parts. *J. Eng.* 2021, 7, 53–69.
68. Hassan, W.; Farid, M.A.; Tosi, A.; Rane, K.; Strano, M. The effect of printing parameters on sintered properties of extrusion-based additively manufactured stainless steel 316L parts. *Int. J. Adv. Manuf. Technol.* 2021, 114, 3057–3067.
69. Henry, T.C.; Morales, M.A.; Cole, D.P.; Shumeyko, C.M.; Riddick, J.C. Mechanical behavior of 17-4 PH stainless steel processed by atomic diffusion additive manufacturing. *Int. J. Adv. Manuf. Technol.* 2021, 114, 2103–2114.
70. Jiang, D.; Ning, F. Additive manufacturing of 316L stainless steel by a printing-debinding-sintering method: Effects of microstructure on fatigue property. *J. Manuf. Sci. Eng.* 2021, 143, 1–30.
71. Mashekov, S.; Bazarbay, B.; Zhankeldi, A.; Masheкова, A. Development of technological basis of 3D printing with highly filled metal-poly-dimensional compositions for manufacture of metal products of complex shape. *Metalurgija* 2021, 60, 355–358.
72. Mousapour, M.; Salmi, M.; Klemettinen, L.; Partanen, J. Feasibility study of producing multi-metal parts by Fused Filament Fabrication (FFF) technique. *J. Manuf. Processes* 2021, 67, 438–446.
73. Quarto, M.; Carminati, M.; D'Urso, G. Density and shrinkage evaluation of AISI 316L parts printed via FDM process. *Mater. Manuf. Processes* 2021, 36, 1535–1543.
74. Quarto, M.; Carminati, M.; D'Urso, G.; Giardini, C.; Maccarini, G. Processability of metal-filament through polymer FDM machine. In *Proceedings of the 24th International Conference on Material Forming*, Liège, Belgium, 14–16 April 2021.

75. Sadaf, M.; Bragaglia, M.; Nanni, F. A simple route for additive manufacturing of 316L stainless steel via Fused Filament Fabrication. *J. Manuf. Processes* 2021, 67, 141–150.
76. Shaikh, M.Q.; Lavertu, P.-Y.; Kate, K.H.; Atre, S.V. Process sensitivity and significant parameters investigation in Metal Fused Filament Fabrication of Ti-6Al-4V. *J. Mater. Eng. Perform.* 2021, 30, 5118–5134.
77. Shaikh, M.Q.; Singh, P.; Kate, K.H.; Freese, M.; Atre, S.V. Finite element-based simulation of metal fused filament fabrication process: Distortion Prediction and Experimental Verification. *J. Mater. Eng. Perform.* 2021, 30, 5135–5149.
78. Singh, P.; Balla, V.K.; Atre, S.V.; German, R.M.; Kate, K.H. Factors affecting properties of Ti-6Al-4V alloy additive manufactured by metal fused filament fabrication. *Powder Technol.* 2021, 386, 9–19.
79. Singh, P.; Balla, V.K.; Gokce, A.; Atre, S.V.; Kate, K.H. Additive manufacturing of Ti-6Al-4V alloy by metal fused filament fabrication (MF3): Producing parts comparable to that of metal injection molding. *Prog. Addit. Manuf.* 2021, 6, 593–606.
80. Tosto, C.; Tirillò, J.; Sarasini, F.; Cicala, G. Hybrid metal/polymer filaments for Fused Filament Fabrication (FFF) to print metal parts. *Appl. Sci.* 2021, 11, 1444.
81. Wang, Y.; Zhang, L.; Li, X.; Yan, Z. On hot isostatic pressing sintering of fused filament fabricated 316L stainless steel—Evaluation of microstructure, porosity, and tensile properties. *Mater. Lett.* 2021, 296, 129854.
82. Lu, Z.; Ayeni, O.I.; Yang, X.; Park, H.-Y.; Jung, Y.-G.; Zhang, J. Microstructure and phase analysis of 3d-printed components using bronze metal filament. *J. Mater. Eng. Perform.* 2020, 29, 1650–1656.
83. Cerejo, F.; Gatões, D.; Vieira, M. Optimization of metallic powder filaments for additive manufacturing extrusion (MEX). *Int. J. Adv. Manuf. Technol.* 2021, 115, 2449–2464.
84. Singh, G.; Missiaen, J.-M.; Bouvard, D.; Chaix, J.-M. Copper extrusion 3D printing using metal injection moulding feedstock: Analysis of process parameters for green density and surface roughness optimization. *Addit. Manuf.* 2021, 38, 101778.
85. Singh, G.; Missiaen, J.-M.; Bouvard, D.; Chaix, J.-M. Copper additive manufacturing using MIM feedstock: Adjustment of printing, debinding, and sintering parameters for processing dense and defectless parts. *Int. J. Adv. Manuf. Technol.* 2021, 115, 449–462.
86. Santos, C.; Gatões, D.; Cerejo, F.; Vieira, T. Influence of metallic powder characteristics on extruded feedstock performance for indirect additive manufacturing. *Materials* 2021, 14, 7136.
87. Vishwanath, A.; Rane, K.; Schaper, J.; Strano, M.; Casati, R. Rapid production of AZ91 Mg alloy by extrusion based additive manufacturing process. *Powder Metall.* 2021, 64, 370–377.

88. Shaikh, M.Q.; Graziosi, S.; Atre, S.V. Supportless printing of lattice structures by metal fused filament fabrication (MF3) of Ti-6Al-4V: Design and analysis. *Rapid Prototyp. J.* 2021, 27, 1408–1422.
89. Terry, S.; Fidan, I.; Tantawi, K. Preliminary investigation into metal-material extrusion. *Prog. Addit. Manuf.* 2021, 6, 133–141.
90. Gonzalez-Gutierrez, J.; Cano, S.; Ecker, J.V.; Kitzmantel, M.; Arbeiter, F.; Kukla, C.; Holzer, C. Bending properties of lightweight copper specimens with different infill patterns produced by material extrusion additive manufacturing, solvent debinding and sintering. *Appl. Sci.* 2021, 11, 7262.
91. Gloeckle, C.; Konkol, T.; Jacobs, O.; Limberg, W.; Ebel, T.; Handge, U.A. Processing of highly filled polymer–metal feedstocks for fused filament fabrication and the production of metallic implants. *Materials* 2020, 13, 4413.
92. Singh, G.; Missiaen, J.-M.; Bouvard, D.; Chaix, J.-M. Additive manufacturing of 17-4 PH steel using metal injection moulding feedstock: Analysis of 3D extrusion printing, debinding and sintering. *Addit. Manuf.* 2021, 47, 102287.
93. Moritzer, E.; Elsner, C.L.; Schumacher, C. Investigation of metal-polymer composites manufactured by fused deposition modeling with regard to process parameters. *Polym. Compos.* 2021, 42, 6065–6079.
94. Hasib, A.G.; Niauzorau, S.; Xu, W.; Niverty, S.; Kublik, N.; Williams, J.; Chawla, N.; Song, K.; Azeredo, B. Rheology scaling of spherical metal powders dispersed in thermoplastics and its correlation to the extrudability of filaments for 3D printing. *Addit. Manuf.* 2021, 41, 101967.
95. Shaikh, M.Q.; Nath, S.D.; Akilan, A.A.; Khanjar, S.; Balla, V.K.; Grant, G.T.; Atre, S.V. Investigation of patient-specific maxillofacial implant prototype development by metal fused filament fabrication (MF3) of Ti-6Al-4V. *Dent. J.* 2021, 9, 109.
96. Naranjo, J.A.; Berges, C.; Gallego, A.; Herranz, G. A novel printable high-speed steel filament: Towards the solution for wear-resistant customized tools by AM alternative. *J. Mater. Res. Technol.* 2021, 11, 1534–1547.
97. Dietrich, S.; Englert, L.; Pinter, P. Non-destructive characterization of additively manufactured components using X-Ray micro-computed tomography. In *Solid Freeform Fabrication Symposium*; University of Texas: Austin, TX, USA, 2018.
98. Rosnitschek, T.; Seefeldt, A.; Alber-Laukant, B.; Neumeyer, T.; Altstädt, V.; Tremmel, S. Correlations of geometry and infill degree of extrusion additively manufactured 316L stainless steel components. *Materials* 2021, 14, 5173.
99. Mohammadzadeh, M.; Lu, H.; Fidan, I.; Tantawi, K.; Gupta, A.; Hasanov, S.; Zhang, Z.; Alifui-Segbaya, F.; Rennie, A. Mechanical and thermal analyses of Metal-PLA components fabricated by

- metal material extrusion. *Inventions* 2020, 5, 44.
100. Jimbo, K.; Tateno, T. Shape contraction in sintering of 3D objects fabricated via metal material extrusion in additive manufacturing. *Int. J. Autom. Technol.* 2019, 13, 354–360.
  101. Zhang, Z.; Femi-Oyetero, J.; Fidan, I.; Ismail, M.; Allen, M. Prediction of dimensional changes of low-cost metal material extrusion fabricated parts using machine learning techniques. *Metals* 2021, 11, 690.
  102. Thompson, Y.; Polzer, M.; Gonzalez-Gutierrez, J.; Kasian, O.; Heckl, J.P.; Dalbauer, V.; Kukla, C.; Felfer, P.J. Fused filament fabrication-based additive manufacturing of commercially pure titanium. *Adv. Eng. Mater.* 2021, 23, 2100380.
  103. Roshchupkin, S.; Golovin, V.; Kolesov, A.; Tarakhovskiy, A.Y. Extruder for the production of metal-polymer filament for additive technologies. In *IOP Conference Series: Materials Science and Engineering*; IOP Publishing: Bristol, UK, 2020; pp. 1–6.
  104. Obadimu, S.O.; McLaughlin, J.; Kourousis, K.I. Immersion ultrasonic testing of artificially induced defects in fused filament fabricated steel 316L. *3D Print. Addit. Manuf.* 2021; in press.
  105. Kan, X.; Yang, D.; Zhao, Z.; Sun, J. 316L FFF binder development and debinding optimization. *Mater. Res. Express* 2021, 8, 116515.
  106. Wagner, M.A.; Hadian, A.; Sebastian, T.; Clemens, F.; Schweizer, T.; Rodriguez-Arbaizar, M.; Carreño-Morelli, E.; Spolenak, R. Fused filament fabrication of stainless steel structures—From binder development to sintered properties. *Addit. Manuf.* 2021, 49, 102472.
  107. Jiang, D.; Ning, F. Anisotropic deformation of 316 L stainless steel overhang structures built by material extrusion based additive manufacturing. *Addit. Manuf.* 2021, 50, 102545.
  108. Santamaria, R.; Salasi, M.; Bakhtiari, S.; Leadbeater, G.; Iannuzzi, M.; Quadir, M.Z. Microstructure and mechanical behaviour of 316L stainless steel produced using sinter-based extrusion additive manufacturing. *J. Mater. Sci.* 2022, 1–17.
  109. Waalkes, L.; Längerich, J.; Imgrund, P.; Emmelmann, C. Piston-based material extrusion of Ti-6Al-4V feedstock for complementary use in metal injection molding. *Materials* 2022, 15, 351.
  110. Suwanpreecha, C.; Manonukul, A. On the build orientation effect in as-printed and as-sintered bending properties of 17-4PH alloy fabricated by metal fused filament fabrication. *Rapid Prototyp. J.* 2022; in press.
  111. Ramazani, H.; Kami, A. Metal FDM, a new extrusion-based additive manufacturing technology for manufacturing of metallic parts: A review. *Prog. Addit. Manuf.* 2022, 1–18.
  112. Hong, S.; Sanchez, C.; Du, H.; Kim, N. Fabrication of 3D printed metal structures by use of high-viscosity Cu paste and a screw extruder. *J. Electron. Mater.* 2015, 44, 836–841.

113. Yan, X.; Hao, L.; Xiong, W.; Tang, D. Research on influencing factors and its optimization of metal powder injection molding without mold via an innovative 3D printing method. *RSC Adv.* 2017, 7, 55232–55239.
114. Rane, K.; Di Landro, L.; Strano, M. Processability of SS316L powder—Binder mixtures for vertical extrusion and deposition on table tests. *Powder Technol.* 2019, 345, 553–562.
115. Rane, K.; Castelli, K.; Strano, M. Rapid surface quality assessment of green 3D printed metal-binder parts. *J. Manuf. Processes* 2019, 38, 290–297.
116. Ren, L.; Zhou, X.; Song, Z.; Zhao, C.; Liu, Q.; Xue, J.; Li, X. Process parameter optimization of extrusion-based 3D metal printing utilizing PW–LDPE–SA binder system. *Materials* 2017, 10, 305.
117. Annoni, M.; Giberti, H.; Strano, M. Feasibility study of an extrusion-based direct metal additive manufacturing technique. *Procedia Manuf.* 2016, 5, 916–927.
118. Rane, K.; Barriere, T.; Strano, M. Role of elongational viscosity of feedstock in extrusion-based additive manufacturing of powder-binder mixtures. *Int. J. Adv. Manuf. Technol.* 2020, 107, 4389–4402.
119. Mishra, A.A.; Momin, A.; Strano, M.; Rane, K. Implementation of viscosity and density models for improved numerical analysis of melt flow dynamics in the nozzle during extrusion-based additive manufacturing. *Prog. Addit. Manuf.* 2022, 7, 41–54.
120. Giberti, H.; Sbaglia, L.; Silvestri, M. Mechatronic design for an extrusion-based additive manufacturing machine. *Machines* 2017, 5, 29.
121. Parenti, P.; Cataldo, S.; Annoni, M. Shape deposition manufacturing of 316L parts via feedstock extrusion and green-state milling. *Manuf. Lett.* 2018, 18, 6–11.
122. Rosnitschek, T.; Glamsch, J.; Lange, C.; Alber-Laukant, B.; Rieg, F. An automated open-source approach for debinding simulation in metal extrusion additive manufacturing. *Designs* 2021, 5, 2.
123. Strano, M.; Rane, K.; Farid, M.A.; Mussi, V.; Zaragoza, V.; Monno, M. Extrusion-based additive manufacturing of forming and molding tools. *Int. J. Adv. Manuf. Technol.* 2021, 117, 2059–2071.
124. Ebel, T. 17—Metal injection molding (MIM) of titanium and titanium alloys. In *Handbook of Metal Injection Molding*; Heaney, D.F., Ed.; Woodhead Publishing: Sawston, UK, 2012; pp. 415–445.
125. Miura, H.; Osada, T.; Itoh, Y. Metal Injection Molding (Mim) Processing. In *Advances in Metallic Biomaterials: Processing and Applications*; Niinomi, M., Narushima, T., Nakai, M., Eds.; Springer: Berlin/Heidelberg, Germany, 2015; pp. 27–56.
126. Ebel, T. Titanium MIM for manufacturing of medical implants and devices. In *Titanium in Medical and Dental Applications*; Elsevier: Amsterdam, The Netherlands, 2018; pp. 531–551.

127. European Powder Metallurgy Association. Metal Injection Moulding: A Manufacturing Process for Precision Engineering Components; European Powder Metallurgy Association: Shrewsbury, UK, 2013.
128. Popescu, D.; Zapciu, A.; Amza, C.; Baciu, F.; Marinescu, R. FDM process parameters influence over the mechanical properties of polymer specimens: A review. *Polym. Test.* 2018, 69, 157–166.
129. Samykano, M.; Selvamani, S.K.; Kadirgama, K.; Ngui, W.K.; Kanagaraj, G.; Sudhakar, K. Mechanical property of FDM printed ABS: Influence of printing parameters. *Int. J. Adv. Manuf. Technol.* 2019, 102, 2779–2796.
130. Wickramasinghe, S.; Do, T.; Tran, P. FDM-based 3D printing of polymer and associated composite: A review on mechanical properties, defects and treatments. *Polymers* 2020, 12, 1529.
131. Turner, B.N.; Strong, R.; Gold, S.A. A review of melt extrusion additive manufacturing processes: I. Process design and modeling. *Rapid Prototyp. J.* 2014, 20, 192–204.
132. Valkenaers, H.; Vogeler, F.; Ferraris, E.; Voet, A.; Kruth, J.-P. A novel approach to additive manufacturing: Screw extrusion 3D-printing. In Proceedings of the 10th International Conference on Multi-Material Micro Manufacture, San Sebastian, Spain, 8–10 October 2013; Research Publishing: Singapore.
133. Bellini, A.; Shor, L.; Guceri, S.I. New developments in fused deposition modeling of ceramics. *Rapid Prototyp. J.* 2005, 11, 214–220.
134. Manonukul, A.; Likityingwara, W.; Rungkiatnawin, P.; Muenya, N.; Amoran, S.; Kittinantapol, W.; Surapunt, S. Study of recycled and virgin compounded metal injection moulded feedstock for stainless steel 630. *J. Solid Mech. Mater. Eng.* 2007, 1, 411–420.
135. AIM3D GmbH Edelstahl. The Next Generation of 3D Printing Advantages of the ExAM 255. Available online: <https://www.aim3d.de/en/products/exam-255/> (accessed on 27 October 2021).
136. Pollen, Ltd. PAM: Pellet Additive Manufacturing. Available online: <https://www.pollen.am/> (accessed on 27 October 2021).
137. Direct3D, Pellet Extrusion. Available online: <https://www.direct3d.it/> (accessed on 27 October 2021).
138. Desktop Metal, Inc. Prototype and Mass Produce with the Same Alloys. Available online: <https://www.desktopmetal.com/products/materials/> (accessed on 27 October 2021).
139. Masood, S.H. Advances in fused deposition modeling. In *Comprehensive Materials Processing*; Elsevier: Amsterdam, The Netherlands, 2014; pp. 69–91.
140. Markforged, Inc. Complete Metal Solution. Available online: <https://markforged.com/metal-x/> (accessed on 27 October 2021).

141. Sargini, M.I.M.; Masood, S.H.; Palanisamy, S.; Jayamani, E.; Kapoor, A. Additive manufacturing of an automotive brake pedal by metal fused deposition modelling. *Mater. Today Proc.* 2021, 45, 4601–4605.
142. Chen, C.L.; Thomson, R.C. Study on thermal expansion of intermetallics in multicomponent Al–Si alloys by high temperature X-ray diffraction. *Intermetallics* 2010, 18, 1750–1757.
143. Turner, B.N.; Gold, S.A. A review of melt extrusion additive manufacturing processes: II. Materials, dimensional accuracy, and surface roughness. *Rapid Prototyp. J.* 2015, 21, 250–261.
144. Ian Gibson, I.G. *Additive Manufacturing Technologies 3D Printing, Rapid Prototyping, and Direct Digital Manufacturing*; Springer: Berlin/Heidelberg, Germany, 2015.
145. Hwang, S.; Reyes, E.I.; Moon, K.-S.; Rumpf, R.C.; Kim, N.S. Thermo-mechanical characterization of metal/polymer composite filaments and printing parameter study for fused deposition modeling in the 3D printing process. *J. Electron. Mater.* 2015, 44, 771–777.
146. The Virtual Foundry, Printing Pure Metal with FILAMET™. Available online: <https://www.thevirtualfoundry.com/help> (accessed on 27 October 2021).
147. Ultrafuse 316L. Available online: <https://www.ultrafuseff.com/product-category/metal/ultrafuse-316l/> (accessed on 27 October 2021).
148. 316L Metal Filament 1.75 mm. Available online: <https://www.anycubic.com/products/316l-metal-filament-1-75mm316L> (accessed on 27 October 2021).

---

Retrieved from <https://encyclopedia.pub/entry/history/show/57056>